Eng. Sci., 2022, **20**, 209–217

Engineered Science

DOI: https://dx.doi.org/10.30919/es8e710

Low Temperature Conversion of Ethane to Ethylene Using Zirconia Supported Molybdenum Oxide Catalysts

A. Sri Hari Kumar,[1,*] Salam K. Al-Dawery,[1] D. Sri Maha Vishnu,[2, 3] V. N. Kalevaru[4] and P. S. Sai Prasad[5]

Abstract

Two series of zirconia supported molybdophosphoric acid (MPA) and MoO_x (ammonium heptamolybdate as precursor) catalysts were synthesized with varying contents of MPA or MoO_x (5-25 wt.%). The catalytic activity was evaluated for oxidative dehydrogenation of ethane (ODHE) to ethylene in a fixed bed catalytic reactor. The Mo oxide phases formed due to the decomposition of MPA during calcination were found to be more active for ODHE than the Mo oxides obtained directly from ammonium heptamolybdate precursor. Brunauer-Emmett-Teller (BET) surface areas and pore volumes are found to depend on Mo loading and varied in the range from 19 to 50 m^2/g. X-ray diffraction (XRD) demonstrates the formation of $Zr(MoO_4)_2$ phase. Fourier transform infrared spectroscopy (FTIR) confirmed the decomposition of MPA after calcination. Catalytic results revealed that the decomposed MPA/ZrO_2 catalysts exhibited better performance compared to MoO_x/ZrO_2 solids with similar Mo contents. It has been observed that Mo loading has shown a clear influence on the catalytic activity and selectivity. Yield of C_2H_4 increased up to 15 wt.% MPA loading and then decreased with further increase in MPA content. Among all catalysts tested, the 15 wt.% MPA/ZrO_2 exhibited the best performance.

Keywords: Ethane; Ethylene; Molybdophosphoric acid; ZrO_2; Oxidative dehydrogenation.
Received: 03 March 2022; Revised: 22 April 2022; Accepted: 28 April 2022.
Article type: Research article.

1. Introduction

Lighter olefins are the building blocks for the production of a good number of commodities in petrochemical industry. In particular, ethylene market is the largest among all olefins. Despite some delays due to COVID-19 crisis, some new cracker projects with roughly 22 million tons (mio. t) of new capacities for ethylene are likely to start in Asia between 2020-22. Recently, the United States has also invested heavily in new cracker projects that accounts to nearly 7.5 mio. t of new ethylene production facilities between 2017-2019. Worldwide market for ethylene is estimated to be 158 mio. t in 2020, which is expected to reach 207 mio. t by 2027.[1] Global demand for ethylene is forecast to grow by about 4% per year, which remains more or less constant for next 7 years (*i.e*. from 2020 to 2027). More than 80% of ethylene is used to produce ethylene oxide, ethylene dichloride, ethyl benzene, polyvinyl chloride and polyethylene. In general, ethylene is produced via steam cracking of gaseous alkanes and liquid petroleum products like naphtha. In the US, ethylene is produced mainly from natural gas-based feedstocks while in Europe and Asia the ethylene productions are largely naphtha-based ones. Steam cracking, which is usually carried out at high temperatures (750 – 950 °C) in tubular reactor made up of heat resistant Fe-Ni-Cr alloys. In ethylene production, more than 10% of ethane is burned to CO_2 alone. Acetylene, higher olefins and coke are some of the other byproducts formed during this synthesis process. However, the amount of coke deposition on the reactor walls depends on the type of feed, operating conditions and alloy composition. Coke accretion on the inner surface of the cracking coil and on transfer line heat exchangers hampers the heat transfer from furnace to the process gas and increase the pressure drop over the coils and ultimately causes frequent plant shutdowns for decoking, thus lowering on-stream time and production capacity. Furthermore, the high temperature combustion also generates huge amounts of NO_x, which are having very high global

[1] *Department of Chemical and Petrochemical Engineering, University of Nizwa, Oman.*
[2] *Department of Biological Sciences and Chemistry, University of Nizwa, Oman.*
[3] *Natural and Medical Sciences Research Center, University of Nizwa, Oman.*
[4] *Leibniz-Institut für Katalyse e.V. an der Universität Rostock, 18059 Rostock, Germany.*
[5] *Center for Chemical Sciences and Technology, Institute of Science & Technology, JNTU, Hyderabad-500085, India.*
**E-mail:* annamareddy@unizwa.edu.om (A. Sri Hari Kumar)

warming potential. The space time was very low usually in the order of milliseconds in order to avoid the formation of CO_x. Moreover, the ethylene yield is typically 30 wt.% with naphtha as feedstock and goes down to 25% for gas oil feedstock.[2]

Ethane is the second abundantly available component in the natural gas having a share of 1-5% in natural gas. The composition of natural gas however varies from region to region. Interestingly, the oxidative dehydrogenation of ethane (ODHE) is thermodynamically favored at low temperatures compared to steam reforming and additionally the presence of O_2 in the reactant feed mixture prevents the coke formation. The design of selective catalyst has got importance due to limited alkene yields (because of over oxidation). Cavani *et al*. have proposed that ethylene yield above 60% is required to compete the steam cracking process.[3] Mo containing catalysts are some of the most effective ones among others for the ODHE of ethane.[4-11] It is well known that the process follows the Mars-van Krevelen mechanism (MVK). According to MVK, the reactant hydrocarbon reduces the catalyst and also reacts with the lattice oxygen and thereby oxygen vacancies are created in the lattice. These oxygen vacancies are replenished by the oxygen present in the gas phase. A variety of catalyst compositions based on Mo,[12] heteropoly compounds,[13] Cr,[14] Ni[15,16] *etc*. were applied by different research groups in recent times to produce ethylene from ODHE. Among different catalyst systems employed, heteropolyacids especially Mo-containing ones show promising catalytic properties. However, their application is limited due to their low thermal stability. In the present study, we have made extensive efforts to explore the potential of decomposed MPA towards ODHE. However, the activity of Mo containing catalysts is strongly related to large number of factors, such as i) the surface composition, ii) the local structure and distribution of dispersed MoO_x species, iii) the nature and identity of the support, iv) the content of Mo and v) the catalyst preparation procedures and source of precursor materials. Some studies have already focused on Mo and V containing catalysts.[17-21] For instance, Christodoulakis *et al*. have studied the zirconia supported molybdena catalysts for ODHE,[22] but the catalytic runs were done at very low reactant concentrations and their work mainly focused on the studies of operando Raman spectroscopy. The aim of the present work is to study the impact of different Mo precursor sources on the catalytic properties of Mo-containing catalysts. Furthermore, special focus was also laid on the activity of decomposed molybdophosphoric acid (MPA) supported on ZrO_2 for the present ODHE and its comparison with that of MoO_x/ZrO_2 catalysts prepared using ammonium heptamolybdate as precursor.

2. Experimental

2.1 Catalyst preparation

Zirconia (ZrO_2) was prepared from Zirconyl nitrate (Sigma Aldrich) by precipitation. 40 grams of $Zr(NO_3)_2$ was dissolved in 400 ml of distilled water. To this, ammonium hydroxide solution (25%) was added drop wise. During the reagents addition the system was kept under constant stirring for 30 min at room temperature. The final pH was adjusted to 9.5 using ammonium hydroxide solution. The solution produced was further stirred for another 12 h and then washed with distilled water using a Buchner funnel until no chloride ions were detected (confirmed from silver nitrate test). The wet solid mass was then dried in an oven at 120 °C for 12 h. Finally, the solid thus obtained was grained and calcined at 600 °C for 6 h in air.

The calculated amounts of (5-25 wt.%) MPA was dissolved in distilled water and to this an appropriate amount of ZrO_2 support was added. The water was evaporated (80 °C) using a hot plate under stirring and then dried in oven for overnight (12 h). The solid mass obtained was calcined at 600 °C for 6 h in air. In a similar way, keeping the Mo content constant to that of the above (5-25wt.% MPA containing catalysts) another series of zirconia supported MoO_x catalysts using ammonium heptamolybdate as Mo precursor were prepared and calcined under the same conditions as above.

2.2 Catalyst characterization

Brunauer-Emmett-Teller (BET) surface areas and pore volume measurements (using Quantachrome 4200e Instrument) of the catalysts were carried out by N_2 adsorption method at -196°C, taking 0.169 nm^2 as the cross-sectional area for di-nitrogen. Before the measurements, the known amount of catalyst was evacuated for 2 h at 200 °C to remove physically adsorbed air and moisture. The pore size distributions of the samples were determined by the BJH (Barett–Joyner–Halenda) model from the data of desorption branch of the nitrogen isotherms.

X-Ray Diffraction (XRD) patterns of the catalysts were obtained with a Rigaku Miniflex (Rigaku Corporation, Japan) X-ray diffractometer using Ni filtered Cu Kα radiation (λ = 1.5406 Å) with a scan speed of 2° min^{-1} and a scan range of 2–80° at 30 kV and 15 mA.

The Raman spectra of the samples were collected on Raman spectrometer system (Horiba-Jobin Yvon LabRam-HR) equipped with a confocal microscope, 2400/900 grooves/mm gratings, and a notch filter. The UV laser excitation at 325 nm was supplied by a Yag doubled-diode pumped laser (20 mW). The scattered photons were directed and focused onto a single-stage monochromator and measured with an UV sensitive LN_2-cooled CCD detector (Jobin Yvon CCD-3000V). The catalyst samples in powder form (about 5–10 mg) were usually loosely spread onto a glass slide below the confocal microscope for Raman measurements.

Temperature programmed reduction (TPR) of the catalysts was carried out in a flow of 5% H_2/Ar mixture gas at a flow rate of 60 ml/min with a temperature ramp of 10 °C /min up to 950 °C. Before the TPR run, the catalysts were pretreated in helium at 100 °C for 2 h. The hydrogen consumption was monitored using a Varian Gas Chromatograph (CP-3800) equipped with thermal conductivity detector.

Fourier Transform Infrared Spectroscopy (FTIR) spectra

were recorded on a DIGILAB (USA) spectrometer, with a resolution of 1 cm^{-1} using KBr disk method.

2.3 Catalytic tests

The catalytic oxidative dehydrogenation of ethane was carried out in a fixed bed down flow reactor (made of SS, length: 300mm, internal diameter: 10mm) at atmospheric pressure. About 1 g of catalyst (sieved fraction of catalyst particle size is in the range from 1 to 1.2 mm) was placed in the reactor using quartz wool plugs. $C_2H_6/O_2/He$ was fed to the reactor with a molar ratio of 15/10/35 and the flow rates of these reactant gases were regulated using mass flow controllers (Alborge). The catalyst bed temperature and reactor skin temperature were monitored. At the reactor outlet, a cold trap was employed to remove the water from the effluent stream. Then the outlet gas after removal of water was analyzed by an on-line using Nucon 5765 Gas Chromatograph equipped with thermal conductivity detector (TCD). O_2 and CO were analysed using a Molecular sieve 5Å (2.5 m) column whereas C_2H_6, C_2H_4 and CO_2 were analysed using a Porapak Q (3 m) column. It should be noted that the blank tests (in absence of catalyst) revealed no conversion of ethane up to 600 °C.

3. Results and discussion

3.1 BET surface areas and pore volumes

BET surface areas and pore volumes of catalysts with different MPA and MoO_x loadings are given in Table 1. The surface area of the pure support (ZrO_2) was also measured and found that it has exhibited the highest surface area (93 m^2/g) compared to the catalysts prepared using this support. The catalysts showed varying surface areas and pore volumes depending upon the content of Mo in the samples. The specific surface areas of the supported catalysts are appreciably lower than the pure support. The surface area of pure ZrO_2 is however decreased considerably after addition of active component (MPA/MoO_x). Mo loading had a clear impact on the surface areas and pore volumes of the samples. The surface areas are observed to decrease from 50.2 to 22.1 m^2/g with increase in MPA loading from 5 to 25 wt.%. On the other hand, in another series the change in surface area varies from 47.1 to 19.2 m^2/g with increase in MoO_x loading from 5 to 25 wt.%. The pore volumes of the catalysts also followed the same decreasing trend with increasing active component in both the series. Between the two, MPA containing catalysts have exhibited slightly higher surface areas and pore volumes compared to equivalent Mo containing MoO_x/ZrO_2 solids. This difference could be due to the formation of in situ decomposed oxides during the calcination of MPA/ZrO_2 samples and hence their catalytic properties might be different from other series of solids.

3.2 X-ray diffraction

The XRD patterns of the fresh catalysts from both the series are shown in Fig. 1a and Fig. 1b. All the catalysts clearly exhibited crystalline nature with a clear domination of monoclinic ZrO_2 phase. In fact, zirconia has exhibited both the monoclinic and tetragonal phases in both the series. However, the ratio of tetragonal to monoclinic phase of zirconia is found to be dependent to some extent on the source of Mo precursor (cf. Fig. 1a and Fig. 1b). XRD patterns also revealed the formation of $Zr(MoO_4)_2$[23] phase in both the catalytic systems (Fig. 1a and Fig. 1b) due to a solid-state reaction between MoO_x and ZrO_2 during thermal treatment (calcination). The intensity of the reflections belonging to this phase is observed to increase continuously with increase in Mo content of the catalysts. On the other hand, no distinct MoO_x and/or P_2O_5 phases were detected by XRD as separate crystalline phases. The non-appearance of reflections corresponding to phosphorous oxide might be due to its presence in negligibly small quantities. The decomposition of MPA into its oxide phase is also revealed by i) the formation of $Zr(MoO_4)_2$ species and ii) absence of characteristic reflections corresponding to Keggin structure. FTIR spectra of MPA/ZrO_2 catalysts shown in Fig. 4 also support this statement. In other words, no IR bands due to Keggin structure are present in all the calcined samples.

Table 1. BET Surface areas and pore volumes of various MPA/ZrO_2 catalysts.

Catalyst	BET-SA (m^2/g)	Pore volume (cm^3/g)	Catalyst	BET-SA (m^2/g)	Pore volume (cm^3/g)
Z	93.0	1.210			
5 MZ	50.2	0.905	5MoZ	47.1	0.896
10MZ	40.9	0.750	10MoZ	36.7	0.690
15MZ	37.1	0.668	15MoZ	32.4	0.581
20MZ	25.7	0.477	20MoZ	23.3	0.421
25MZ	22.1	0.409	25MoZ	19.2	0.342

Z = ZrO_2, MZ = MPA/ZrO_2 solids; MoZ = MoO_x/ZrO_2 samples.

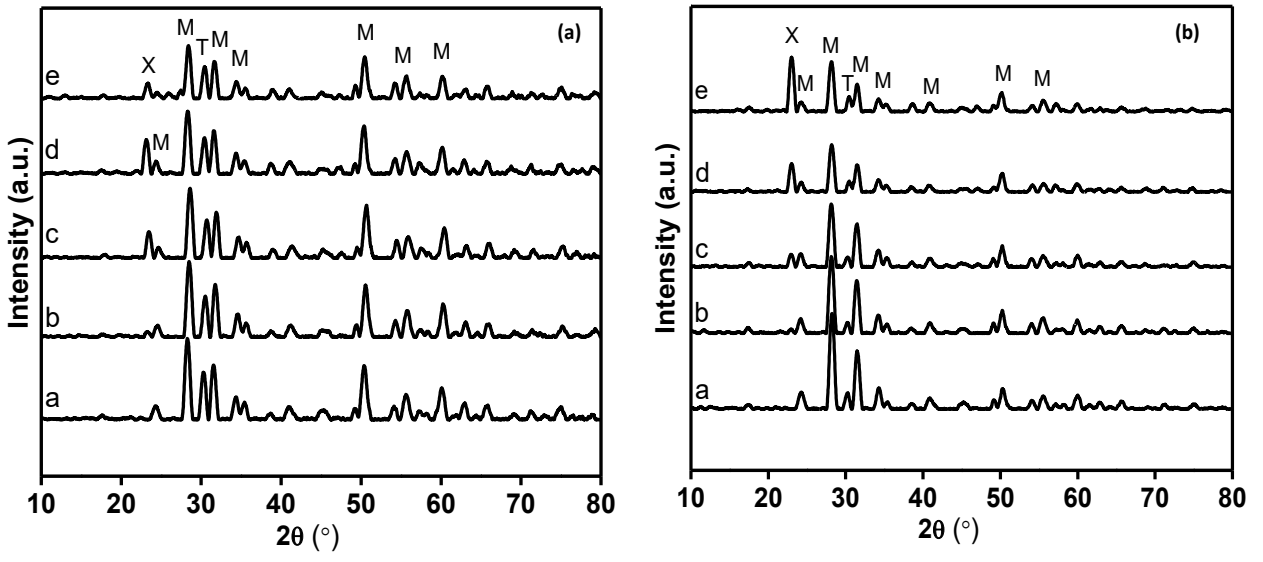

Fig. 1 a) XRD patterns of ZrO_2 supported molybdophosphoric acid catalysts. (a) 5 wt.% MPA/ZrO_2; (b) 10 wt.% MPA/ZrO_2; (c) 15 wt.% MPA/ZrO_2; (d) 20 wt.% MPA/ZrO_2; (e) 25 wt.% MPA/ZrO_2; (X-$Zr(MoO_4)_2$, M-Monoclinic phase of zirconia, T-Tetragonal phase of zirconia), b) XRD patterns of ZrO_2 supported MoO_x catalysts. (a) 5 wt.% MoO_x/ZrO_2; (b) 10 wt.% MoO_x/ZrO_2; (c) 15 wt.% MoO_x/ZrO_2; (d) 20 wt.% MoO_x/ZrO_2; (e) 25 wt.% MoO_x/ZrO_2; (X-$Zr(MoO_4)_2$, M-Monoclinic phase of zirconia, T-Tetragonal phase of zirconia).

3.3 Laser Raman spectroscopy

Figure 2a shows Raman spectra obtained for the MPA/ZrO_2 samples studied at 25°C. The Raman bands due to dispersed surface molybdena (α-MoO_3) were observed at 993 cm^{-1}. However, this band at 993 cm^{-1} is not witnessed up to 15 wt.% MPA loading but thereafter an increase in intensity is observed. The characteristic bands due to $Zr(MoO_4)_2$ were seen at 471, 743 and a weak band at 941 cm^{-1} (Fig. 2a). Xie *et al*. reported that Mo^{6+} cations present in $Zr(MoO_4)_2$ phase are in a distorted tetrahedral coordination with one oxygen bonded only to molybdenum and the other three shared by Zr and Mo atoms.[24] The authors also claimed that the bridging O atoms in Mo-O-Mo species exchanged with gas phase $^{18}O_2$ more readily than terminal Mo=O species. XRD patterns also confirmed the formation of $Zr(MoO_4)_2$ phase in the catalysts. The Raman band at 818 cm^{-1} can be assigned to the stretching vibrations of Mo-O-Mo units.[22,25,26] Another band appeared at 993 cm^{-1} can be attributed to ν(Mo=O) vibrational mode. The bands appeared at 194 and 335 cm^{-1} correspond to Zr-Zr vibrations.[27] These two bands are seemed to be shifted to lower wavenumbers and appeared at 188 and 326 cm^{-1} in MoO_x/ZrO_2 solids shown below in Fig. 2b.

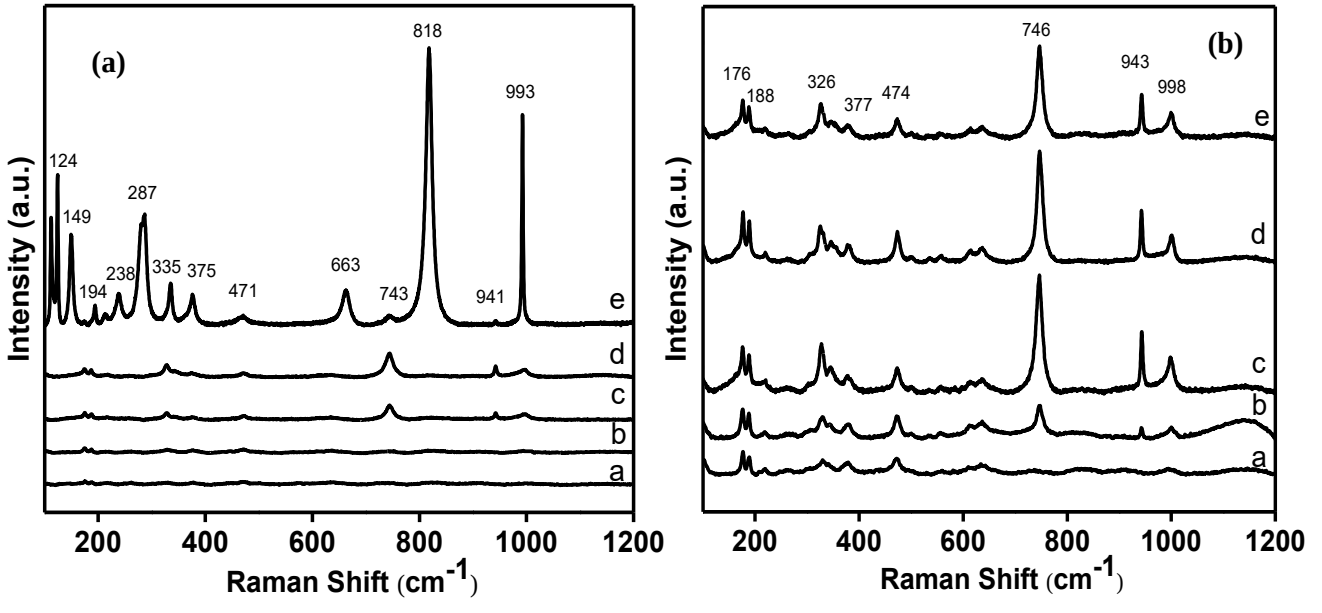

Fig. 2 a) Raman spectra patterns of ZrO_2 supported MPA catalysts. (a) 5 wt.% MPA/ZrO_2; (b) 10 wt.% MPA/ZrO_2; (c) 15 wt.% MPA/ZrO_2; (d) 20 wt.% MPA/ZrO_2; (e) 25 wt.% MPA/ZrO_2; b) Raman spectra patterns of ZrO_2 supported MoO_x catalysts. (a) 5 wt.% MoO_x/ZrO_2; (b) 10 wt.% MoO_x/ZrO_2; (c) 15 wt.% MoO_x/ZrO_2; (d) 20 wt.% MoO_x/ZrO_2; (e) 25 wt.% MoO_x/ZrO_2.

Figure 2b depicts the Raman spectra of MoO_x/ZrO_2 solids. The Raman spectra of these catalysts are seemingly different to the spectra of MPA/ZrO_2 samples. Relatively intense bands could be seen in all the loadings of MoO_x/ZrO_2 solids. However, no crystalline reflections correspond to MoO_x phase could be seen from XRD patterns. Therefore, it seems that such MoO_x phase formed might be X-ray amorphous in nature. The Raman bands at 176, 188 and 474 cm^{-1} were the result of monoclinic phase of zirconia in MoO_x/ZrO_2 catalysts (Fig. 2b).[28] In contrast, non-appearance of monoclinic or tetragonal zirconia phases could be seen in MPA/ZrO_2 samples probably due to well dispersion of MPA at lower loadings and the formation of $Zr(MoO_4)_2$ at higher MPA loadings (Fig. 2a). The formation of $Zr(MoO_4)_2$ phase was observed in MoO_x/ZrO_2 catalysts also at 746 and 943 cm^{-1} (Fig. 2b). The Raman band appeared at 998 cm^{-1} is due to ν(Mo=O) vibrations.

3.4 H_2-Temperature programmed reduction

Temperature programmed reduction (TPR) profiles of ZrO_2 supported MPA and MoO_x catalysts are displayed in Fig. 3a and Fig. 3b. The measurements were recorded up to 950 °C and no reduction of either monoclinic or tetragonal zirconia was observed.[29] The reduction of molybdena can essentially take place in two steps starting from +6 to +4 and +4 to 0. The H_2 consumption is found to increase with Mo loading. The reduction profiles of the catalysts consist of two maxima, *i.e.* one in the range from 400 °C to 650 °C and the other at > 800 °C. The TPR profiles of MPA/ZrO_2 and MoO_x/ZrO_2 catalyst series revealed that the T_{max} value of the first reduction peak was found to shift gradually to higher temperature with the increase of Mo loading above 10 wt.%. The first reduction peak (400 – 620 °C) could be assigned to the reduction of octahedral molybdena (*i.e.* Mo^{6+} to Mo^{4+}) whereas the second reduction peak (T > 800 °C) could be due to the reduction of tetrahedral species (Mo^{4+} to Mo^0). Most of the MPA/ZrO_2 catalysts have undergone reduction mainly in two steps however the reduction of 20 and 25 wt.% MoO_x/ZrO_2 catalysts seems to be reduced virtually in single stage from Mo^{6+} to Mo^0 in the temperature range of 450 to 700 °C (cf. Fig. 3a and Fig. 3b). Relatively high H_2-uptake is evidenced by enhanced reduction peaks in MPA/ZrO_2 solids compared to MoO_x/ZrO_2 samples.

3.5 Fourier transform infrared spectroscopy

The FTIR spectra of ZrO_2 supported MPA catalysts are shown in Fig. 4. Spectra of pure MPA was also presented for better comparison. The decomposition of Keggin structure (the absence of 1064, 960, 870 cm^{-1} and a broad band at 783 cm^{-1}) in MPA containing catalysts was confirmed from FTIR. This result is also in line with the results obtained from XRD and Laser Raman spectroscopy. The IR spectra of MPA/ZrO_2 catalysts exhibited bands in the range of 900 – 450 cm^{-1}. The peaks corresponding to the vibration of Mo-O bonds are expected to appear in the range of 600 and 500 cm^{-1}, but these bands are overlapped with that of ZrO_2. The bands seen for MPA/ZrO_2 catalysts are mainly due to ZrO_2. However, the decomposition of Keggin structure of MPA in the catalysts was clearly observed.

3.6 Catalytic results

The Fig. 5 depicts the influence of MPA loading on ethane conversion at different temperatures namely 450, 500 and 550 °C. The content of MPA has shown a strong influence on the activity of the catalysts. The conversion of ethane was found to be decreasing with the increase in MPA loading. This effect was clearly observed at the highest temperature, *i.e.* at 550 °C. 5 wt.% MPA/ZrO_2 catalyst has displayed the highest ethane conversion of 36.5% among others. From this study, it is observed that a reaction temperature of 550 °C is required to obtain acceptably high conversion of ethane. It should be noted that between the two series tested, MPA/ZrO_2 exhibited better performance compared to MoO_x/ZrO_2 catalysts. Fig. 6

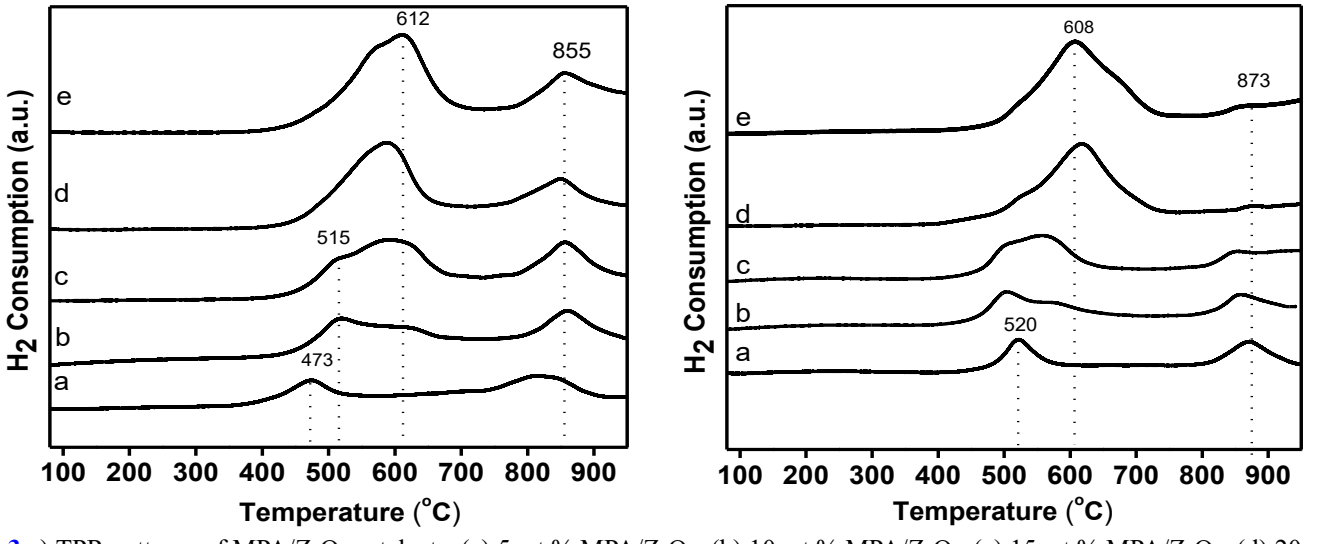

Fig. 3 a) TPR patterns of MPA/ZrO_2 catalysts. (a) 5 wt.% MPA/ZrO_2; (b) 10 wt.% MPA/ZrO_2; (c) 15 wt.% MPA/ZrO_2; (d) 20 wt.% MPA/ZrO_2; (e) 25 wt.% MPA/ZrO_2; b) TPR patterns of MoO_x/ZrO_2 catalysts. (a) 5 wt.% MoO_x/ZrO_2; (b) 10 wt.% MoO_x/ZrO_2; (c) 15 wt.% MoO_x/ZrO_2; (d) 20 wt.% MoO_x/ZrO_2; (e) 25 wt.% MoO_x/ZrO_2.

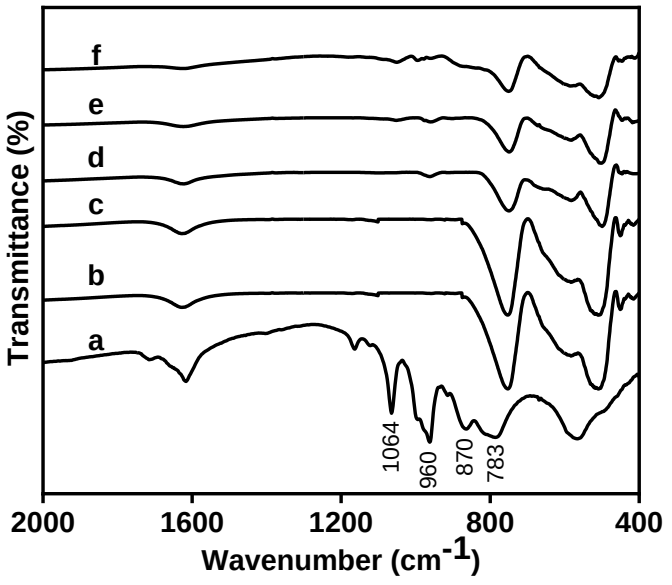

Fig. 4 The FTIR spectra of ZrO_2 supported MPA catalysts. (a) pure MPA, (b) 5 wt.% MPA/ZrO_2, (c) 10 wt.% MPA/ZrO_2, (d) 15 wt.% MPA/ZrO_2, (e) 20 wt.% MPA/ZrO_2, (f) 25 wt.% MPA/ZrO_2.

presents the results from the effect of MPA loading on ethane conversion, selectivity and yield of ethylene obtained at highest reaction temperature (550 °C), where the catalyst displayed better performance. At low MPA contents, even though the conversion of ethane is relatively high but the selectivity towards ethylene is low. It is evident from Fig. 6 that the conversion of ethane decreased from 37% to 18% with increase in MPA loading from 5 to 25 wt.%. Even though the conversion decreased with the loading, the ethylene selectivity was found to increase up to 15 wt.% MPA/ZrO_2.

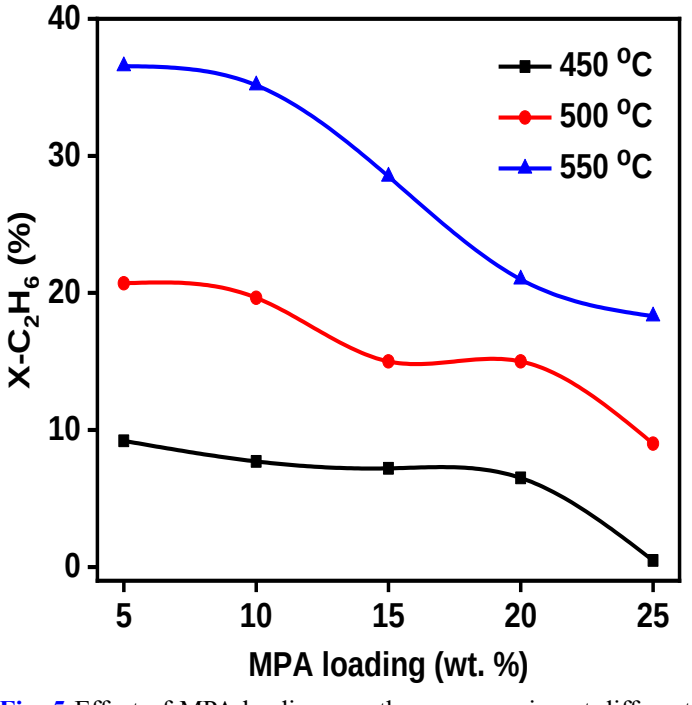

Fig. 5 Effect of MPA loading on ethane conversion at different temperatures.

In other words, 15 wt.% MPA/ZrO_2 catalyst has exhibited the highest ethylene selectivity and also yield among all the catalysts tested. Such increase in selectivity could be attributed to the formation of $Zr(MoO_4)_2$ phase, whose formation could be clearly identified from XRD. The $Zr(MoO_4)_2$ phase could not be seen in the lower loadings of MPA/ZrO_2 catalysts, which might be the reason for low selectivity of ethylene. Ethylene is the major product, while CO_2 and CO are the other by-products. The highest selectivity of C_2H_4 >55%) could be achieved on 15 wt.% MPA/ZrO_2 catalyst (Fig. 6). The best optimum seems to be 15 wt.% MPA/Al_2O_3, where the highest yield of ethylene (Y-C_2H_4 = 15.9%) could be obtained.

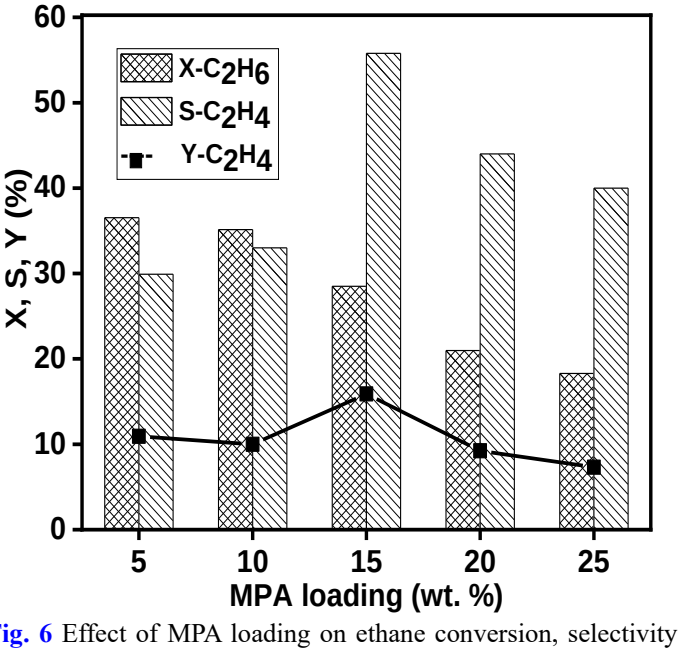

Fig. 6 Effect of MPA loading on ethane conversion, selectivity and yield of ethylene at 550 °C.

Additionally, the activity data obtained over MoO_x/ZrO_2 catalysts at 550 °C was also presented for better comparison. The Fig. 7 illustrates the influence of MoO_x solids derived from ammonium heptamolybdate precursor on ethane conversion, ethylene selectivity and yield of ethylene and CO_2. The conversion of ethane and CO_2 yield are maintained more or less constant up to 15% MoO_x/ZrO_2 catalyst and then decreased thereafter. The CO_2 yield was always higher than that of C_2H_4 yield in these catalysts. No significant change in the C_2H_4 yield was observed with change in MoO_x loading. The MPA containing catalysts have shown superior activity and selectivity compared to MoO_x containing catalysts. The Mo oxides derived from the in-situ decomposition of MPA are relatively active compared to that of Mo derived using other precursors. The study conducted by Sri Hari *et al.* on Mo oxides derived from MPA also revealed similar results.[30,31] Christodoulakis *et al.* explained the activity and molecular structure of zirconia supported molybdena catalysts for ethane oxidative dehydrogenation using operando Raman spectroscopy.[22] They also claimed that with the increased loading of MoO_x, the Mo=O sites would be perturbed and

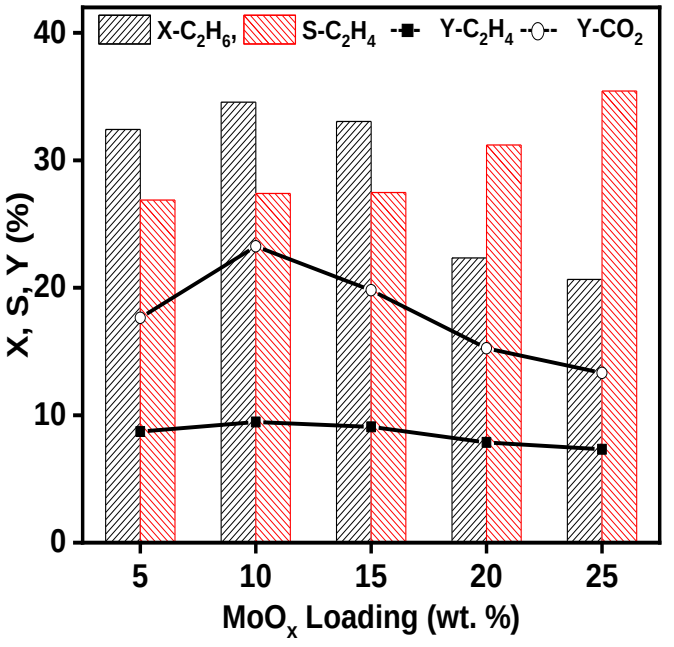

Fig. 7 Effect of MoO_x loading on ethane conversion, selectivity and yield of ethylene at 550 °C.

reduced to a greater extent compared with Mo-O-Mo.[22] The maximum ethane conversion of ~20% was only reported by them at a temperature of 540 °C on zirconia supported molybdena catalysts. It was also suggested that the initial selectivity to C_2H_4 and CO_x were found to be a function of Mo surface density.[22] The relatively high surface area, in-situ generated Mo oxides, the efficient redox properties has made the present MPA/ZrO_2 catalysts as superior catalysts compared to MoO_x/ZrO_2 catalysts.

4. Conclusions

Two series of zirconia supported molybdophosphoric acid (MPA) and MoO_x (ammonium heptamolybdate as precursor) catalysts were synthesized with varying contents of MPA or MoO_x (5-25 wt.%). The Mo oxide phases formed due to the decomposition of MPA during calcination were found to be active for ODHE than Mo oxides obtained from ammonium heptamolybdate. MPA derived catalysts displayed relatively higher surface areas and pore volumes compared to the other series of catalysts. Catalytic results showed that the MPA/ZrO_2 catalysts gave better performance than MoO_x/ZrO_2 solids. Decomposition of MPA has led to the formation of mixed oxides. The intensities of monoclinic and tetragonal phases were found to depend on the source of Mo. Among all catalysts tested, the 15 wt.% MPA/ZrO_2 exhibited the highest ethylene yield.

Acknowledgments

The authors thank University of Nizwa for providing their support in catalyst preparation and catalyst characterization. The authors thank The Research Council (TRC) of Oman, for providing the financial support (Project ID: BFR/RGP/EI/18/023) to conduct the current research.

Conflict of Interest

The authors declare no conflict of interest.

Supporting information

Not applicable.

References

[1] H. Xing, X. Zhao, Q. Yang, B. Su, Z. Bao, Y. Yang, Q. Ren, Molecular dynamics simulation study on the absorption of ethylene and acetylene in ionic liquids, *Industrial & Engineering Chemistry Research*, 2013, **52**, 9308-9316, doi: 10.1021/ie400999f.

[2] J. Towfighi, H. Zimmermann, R. Karimzadeh, M. M. Akbarnejad, Steam cracking of naphtha in packed bed reactors, *Industrial & Engineering Chemistry Research*, 2002, **41**, 1419-1424, doi: 10.1021/ie010636e.

[3] F. Cavani, N. Ballarini, A. Cericola, Oxidative dehydrogenation of ethane and propane: how far from commercial implementation?, *Catalysis Today*, 2007, **127**, 113-131, doi: 10.1016/j.cattod.2007.05.009.

[4] A. Christodoulakis, E. Heracleous, A. Lemonidou, S. Boghosian, An operando Raman study of structure and reactivity of alumina-supported molybdenum oxide catalysts for the oxidative dehydrogenation of ethane, *Journal of Catalysis*, 2006, **242**, 16-25, doi: 10.1016/j.jcat.2006.05.024.

[5] G. Tsilomelekis, A. Christodoulakis, S. Boghosian, Support effects on structure and activity of molybdenum oxide catalysts for the oxidative dehydrogenation of ethane, *Catalysis Today*, 2007, **127**, 139-147, doi: 10.1016/j.cattod.2007.03.026.

[6] A. Simon, E. V. Kondratenko, Investigation of the electrical and catalytic properties of materials with $Cs_x(Mo, Nb)_5O_{14}$ composition, *Applied Catalysis A: General*, 2011, **392**, 199-207, doi: 10.1016/j.apcata.2010.11.015.

[7] G. Tsilomelekis, S. Boghosian, Structural and vibrational properties of molybdena catalysts supported on alumina and zirconia studied by *in situ* Raman and FTIR spectroscopies combined with 180/160 isotopic substitution, *Catalysis Today*, 2010, **158**, 146-155, doi: 10.1016/j.cattod.2010.06.026.

[8] T. D. Nguyen, W. Zheng, F. E. Celik, G. Tsilomelekis, CO_2-assisted ethane oxidative dehydrogenation over MoO_x catalysts supported on reducible CeO_2-TiO_2, *Catalysis Science & Technology*, 2021, **11**, 5791-5801, doi: 10.1039/d1cy00362c.

[9] P. Novotný, S. Yusuf, F. Li, H. H. Lamb, Oxidative dehydrogenation of ethane using MoO_3/Fe_2O_3 catalysts in a cyclic redox mode, *Catalysis Today*, 2018, **317**, 50-55, doi: 10.1016/j.cattod.2018.02.046.

[10] S. Qian, Y. Chen, B. Yan, Y. Cheng, Plasma treated M1 MoVNbTeO-CeO_2 composite catalyst for improved performance of oxidative dehydrogenation of ethane, *Green Energy & Environment*, 2022, doi: 10.1016/j.gee.2022.01.001.

[11] D. Pan, F. Su, C. Liu, Z. Guo, Research progress for plastic waste management and manufacture of value-added products, *Advanced Composites and Hybrid Materials*, 2020, **3**, 443-461,

doi: 10.1007/s42114-020-00190-0.
[12] P. Novotný, S. Yusuf, F. Li, H. H. Lamb, MoO_3/Al_2O_3catalysts for chemical-looping oxidative dehydrogenation of ethane, *The Journal of Chemical Physics*, 2020, **152**, 044713, doi: 10.1063/1.5135920.
[13] S. A. Tungatarova, D. B. Abdukhalykov, T. S. Baizhumanova, L. V. Komashko, V. P. Grigorieva, I. S. Chanysheva, Oxidation of alkanes into olefins on the polyoxide catalysts, *Catalysis Today*, 2015, **256**, 276-286, doi: 10.1016/j.cattod.2015.03.004.
[14] A. Al-Mamoori, S. Lawson, A. A. Rownaghi, F. Rezaei, Oxidative dehydrogenation of ethane to ethylene in an integrated CO_2 capture-utilization process, *Applied Catalysis B: Environmental*, 2020, **278**, 119329, doi: 10.1016/j.apcatb.2020.119329.
[15] E. Rodríguez-Castellón, D. Delgado, A. Dejoz, I. Vázquez, S. Agouram, J. A. Cecilia, B. Solsona, J. M. López Nieto, Enhanced NiO dispersion on a high surface area pillared heterostructure covered by niobium leads to optimal behaviour in the oxidative dehydrogenation of ethane, *Chemistry*, 2020, **26**, 9371-9381, doi: 10.1002/chem.202000832.
[16] Y. Abdelbaki, A. de Arriba, B. Solsona, D. Delgado, E. García-González, R. Issaadi, J. M. López Nieto, The nickel-support interaction as determining factor of the selectivity to ethylene in the oxidative dehydrogenation of ethane over nickel oxide/alumina catalysts, *Applied Catalysis A: General*, 2021, **623**, 118242, doi: 10.1016/j.apcata.2021.118242.
[17] F. Rahman, K. F. Loughlin, M. A. Al-Saleh, M. R. Saeed, N. M. Tukur, M. M. Hossain, K. Karim, A. Mamedov, Kinetics and mechanism of partial oxidation of ethane to ethylene and acetic acid over MoV type catalysts, *Applied Catalysis A: General*, 2010, **375**, 17-25, doi: 10.1016/j.apcata.2009.11.026.
[18] T. Y. Kardash, L. M. Plyasova, V. M. Bondareva, T. V. Andrushkevich, L. S. Dovlitova, A. I. Ischenko, A. I. Nizovskii, A. V. Kalinkin, $M5O_{14}$-like V-Mo-Nb oxide catalysts: structure and catalytic performance, *Applied Catalysis A: General*, 2010, **375**, 26-36, doi: 10.1016/j.apcata.2009.12.003.
[19] J. M. López Nieto, B. Solsona, P. Concepción, F. Ivars, A. Dejoz, M. I. Vázquez, Reaction products and pathways in the selective oxidation of C2-C4 alkanes on MoVTeNb mixed oxide catalysts, *Catalysis Today*, 2010, **157**, 291-296, doi: 10.1016/j.cattod.2010.01.046.
[20] I. P. Belomestnykh, G. V. Isaguliants, S. P. Kolesnikov, V. P. Danilov, O. N. Krasnobaeva, T. A. Nosova, T. A. Elisarova, V-Mo-Nb-W-containing hydrotalcite-like materials as precursors of catalysts for oxidative dehydrogenation of hydrocarbons and alcohols, *Studies in Surface Science and Catalysis*, 2010, **175**, 413-416, doi: 10.1016/S0167-2991(10)75073-4.
[21] G. A. Zenkovets, V. M. Bondareva, A. A. Shutilov, V. I. Sobolev, A. S. Marchuk, S. V. Tsybulya, I. P. Prosvirin, E. A. Suprun, A. V. Ishchenko, V. Y. Gavrilov, Multicomponent $MoVSbNbGdO_x/SiO_2$ catalyst in oxidative dehydrogenation of ethane: effect of Gd on catalytic properties, *Applied Catalysis A: General*, 2022, **633**, 118536, doi: 10.1016/j.apcata.2022.118536.
[22] A. Christodoulakis, S. Boghosian, Molecular structure and activity of molybdena catalysts supported on zirconia for ethane oxidative dehydrogenation studied by operando Raman spectroscopy, *Journal of Catalysis*, 2008, **260**, 178-187, doi: 10.1016/j.jcat.2008.09.025.
[23] J. R. Sohn, J. S. Han, J. S. Lim, Spectroscopic study of V_2O_5 supported on zirconia and modified with MoO_3, *Materials Chemistry and Physics*, 2005, **91**, 558-566, doi: 10.1016/j.matchemphys.2004.12.024.
[24] S. Xie, K. Chen, A. T. Bell, E. Iglesia, Structural characterization of molybdenum oxide supported on zirconia, *The Journal of Physical Chemistry B*, 2000, **104**, 10059-10068, doi: 10.1021/jp002419h.
[25] B. C. Windom, W. G. Sawyer, D. W. Hahn, A Raman spectroscopic study of MoS_2 and MoO_3: applications to tribological systems, *Tribology Letters*, 2011, **42**, 301-310, doi: 10.1007/s11249-011-9774-x.
[26] L. Seguin, M. Figlarz, R. Cavagnat, J.-C. Lassègues, Infrared and Raman spectra of MoO_3 molybdenum trioxides and $MoO_3 \cdot xH_2O$ molybdenum trioxide hydrates, *Spectrochimica Acta Part A: Molecular and Biomolecular Spectroscopy*, 1995, **51**, 1323-1344, doi: 10.1016/0584-8539(94)00247-9.
[27] B.-K. Kim, H.-O. Hamaguchi, Mode assignments of the Raman spectrum of monoclinic zirconia by isotopic exchange technique, *Physica Status Solidi (b)*, 1997, **203**, 557-563, doi: 10.1002/1521-3951(199710)203: 2557: aid-pssb557>3.0.co;2-c.
[28] P. Barberis, T. Merle-Méjean, P. Quintard, On Raman spectroscopy of zirconium oxide films, *Journal of Nuclear Materials*, 1997, **246**, 232-243, doi: 10.1016/s0022-3115(97)00038-x.
[29] C. Liu, W. Wang, Y. Xu, Z. Li, B. Wang, X. Ma, Effect of zirconia morphology on sulfur-resistant methanation performance of MoO_3/ZrO_2 catalyst, *Applied Surface Science*, 2018, **441**, 482-490, doi: 10.1016/j.apsusc.2018.02.019.
[30] A. S. H. Kumar, K. Upendar, A. Qiao, P. S. N. Rao, N. Lingaiah, V. N. Kalevaru, A. Martin, C. Sailu, P. S. S. Prasad, Selective oxidative dehydrogenation of ethane over MoO_3/V_2O_5-Al_2O_3 catalysts: heteropolymolybdate as a precursor for MoO_3, *Catalysis Communications*, 2013, **33**, 76-79, doi: 10.1016/j.catcom.2012.12.012.
[31] A. Sri Hari Kumar, V. N. Kalevaru, A. Qiao, A. Alshammari, N. Lingaiah, C. Sailu, P. S. Sai Prasad, A. Martin, Catalytic behavior of decomposed molybdophosphoric acid supported on alumina for oxidative dehydrogenation of ethane to ethylene, *Kinetics and Catalysis*, 2013, **54**, 615-619, doi: 10.1134/s002315841305008x.

Author Information

A. Sri Hari Kumar *has carried out his doctoral research at Indian Institute of Chemical Technology, India on "Catalytic Transformations of Ethane (Oxidative Dehydrogenation)" his Ph.D. degree in Chemical Engineering from Osmania University, India in 2014. Then he worked as an assistant Professor at Adama Science and Technology*

University of Ethiopia from 2013 to 2015, Defence Engineering College of Ethiopia from 2015 to 2016. Since 2016 to date, he is working as Assistant Professor and Head of the Department at University of Nizwa, Sultanate of Oman. His research interests include catalyst synthesis, characterisation, and catalyst evaluation in fixed bed reactors under gas phase conditions catalysis. His research interests also include chemical reaction engineering, wastewater treatment, and waste to value added materials. He has managed to secure 3 research projects and holds 22 publications in the field of catalysis, water treatment.

***Salam K. Al-Dawery**, received his BSc in chemical engineering at University of Baghdad, Iraq in 1985 and he received his master's degree (1988) and PhD degree (1991) in Chemical Engineering at Nottingham University, U.K. Then, he joined Iraqi atomic energy commission, Iraq in 1991 to 1993 as senior engineer. He has worked as an associate Prof. of Chemical Engineering at the University of Baghdad from 1993 to 2007. He worked as an associate Prof. of Chemical Engineering at the University of Sohar from 2007 to 2009. Since 2009 to date, he is working as an associate Prof. of Chemical Engineering and assistant dean for research at the University of Nizwa, Sultanate of Oman. His research interest: process control, process modeling and wastewater treatment and rheology. He supervised many Master and PhD theses and graduation projects. He has more than 83 publications. He managed to secure 10 funded research projects. He awarded by the president of Majlis Al Shura in the Sultanate of Oman in 2017 for his contribution to legislation a law for treatment and re-use of wastewater and he has many other best research papers. Chairman of the organization committee for 3rd – 10th of National Symposium on Engineering Final Year Projects (2013-2020).*

***D. Sri Maha Vishnu** is currently working as Assistant Professor with the Department of Biological Sciences and Chemistry (DBSC), University of Nizwa. He obtained his Ph.D. in Chemistry from Homi Bhabha National Institute (HBNI), India in 2014. He did his postdoc at the Department of Materials Science and Metallurgy, University of Cambridge, UK from 17/11/2014 to 07/09/2018 during which he has worked on the various collaborative research projects of University of Nizwa and the University of Cambridge. He has published 30 research articles in renowned international journals and presented his work at 24 national and international conferences. Currently he has been working on the synthesis and characterisation of nanomaterials, biomedical alloys and composite materials. In addition, he is also working on various R&D projects related to the aqueous and non-aqueous electrochemistry, electrometallurgy and corrosion.*

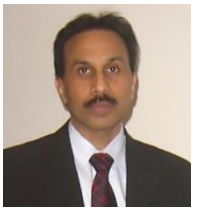

***Venkata Narayana Kalevaru** has carried out his doctoral research at Indian Institute of Chemical Technology, India on the ammoxidation of hetero aromatics and received his Ph.D. degree in Chemistry (Heterogeneous Catalysis) from Osmania University, India in 1998. Then he joined Institute for Applied Chemistry, Berlin in 2000 as a scientist dealing with various basic and industrial projects. Presently, he is a senior Scientist in the Department of Heterogeneous Catalytic processes, Leibniz institute for Catalysis, Rostock, Germany. His research interests include catalyst synthesis, characterisation and catalyst evaluation in fixed bed reactors under gas phase conditions. Some specific examples for instance are, selective oxidations, ammoxidation aromatics / heteroaromatics, oxy-chlorinations, acetoxylation of aromatics, hydroxylation of benzene to phenol, natural gas and CO_2 utilisation, synthesis of bio-based nylon intermediates from the transesterification of gamma-valerolactone with methanol etc. are some of his key research areas. He holds >30 patents and ca. 120 publications in the field of catalysis.*

***P. S. Sai Prasad** has carried out his doctoral research at Indian Institute of Technology-Madras, India and received his Ph.D. degree in Chemical Engineering in 1993. He worked as a Scientist, Chief Scientist, Emeritus Scientist in Indian Institute of Chemical Technology, India. His research interests include catalyst synthesis, characterisation, and catalyst evaluation. He holds 16 patents and 200 publications in the field of catalysis and chemical engineering.*

Publisher's Note: Engineered Science Publisher remains neutral with regard to jurisdictional claims in published maps and institutional affiliations.